JOURNAL OF SOLID STATE CHEMISTRY **141,** 235–240 (1998)
ARTICLE NO. SC987964

Kinetics of Oxidation of Fuel Cell Cathode Materials Lanthanum Strontium Manganates(III)(IV) at Actual Working Conditions: *In Situ* Powder Diffraction Studies

E. Krogh Andersen[1] and I. G. Krogh Andersen

Department of Chemistry, Odense University, DK-5230 Odense M, Denmark

and

P. Norby and J. C. Hanson

Chemistry Department Brookhaven National Laboratory, Upton, New York, 11973

Received March 12, 1998; accepted June 25, 1998

Time resolved synchrotron X-ray powder diffraction methods have been used to study the kinetics of oxidation of lanthanum strontium manganates(III, IV) in a flow of oxygen. The process studied is $La_{1-x}Sr_xMnO_{3.00} + \delta/2 O_2 \leftrightarrow La_{1-x}Sr_xMnO_{3.00+\delta}$ (for $x = 0.00, 0.10, 0.15$). A contraction of the unit cell is observed on oxidation of the materials. The unit cell volume changes linearly with the mean oxidation state of the manganese. Rate constants for the process can consequently be determined from time resolved X-ray diffractograms. The reactions follow first-order kinetics. Arrhenius plots based on rate constants determined at 4 temperatures in the range 700–900°C are linear as an indication that only one rate determining step is involved. The activation energy for oxidation is 136 kJmol^{-1} for $LaMnO_{3.00}$, 179 kJmol^{-1} for $La_{0.90}Sr_{0.10}Mn_{1.01}O_{3.01}$, and 160 kJmol^{-1} for $La_{0.84}Sr_{0.15}Mn_{1.01}O_{3.00}$.

INTRODUCTION

Strontium substituted lanthanum manganates(III)(IV), $La_{1-x}Sr_xMnO_{3+\delta}$ (LSM) are cathode materials for high temperature solid oxide fuel cells/SOFC. They act in the cells as catalysts for the reduction of oxygen, as oxygen ion conductors, and as electronic conductors. The high temperature fuel cell works at temperatures close to 1000°C in surroundings of varying oxygen partial pressures. It is therefore important to study the redox properties of the materials at high temperatures. Kinetic studies of gas/solid reactions have traditionally been performed using thermogravimetric or volumetric methods. However, by using diffraction methods in kinetic analyses, the information obtained is directly related to the material. A unique feature of *in situ* time resolved powder diffraction is that it is possible to obtain structural and kinetic information for the solid materials under actual working conditions. Three conditions are of supreme importance for kinetic studies of reactions between solids and gases by crystallographic means. The reaction should be studied *in situ*, the samples should be small to ensure that change of gas is fast throughout the entire sample, and structural data should be extracted using very short exposures. *In situ* X-ray synchrotron radiation powder diffraction provide optimum conditions on all three points. Our investigation is as far as we know the first crystallographic study of the kinetics of an oxidation of a solid.

Lanthanum manganates and strontium substituted lanthanum manganates have distorted perovskite-type structures and contain manganese in oxidation states III and IV. The formulae of the materials may be written $La_{1-x}Sr_xMn(III)_yMn(IV)_zO_{3+\delta}$. As the chemical analyses showed that $y + z = 1$ for the samples, we will use the simpler formula $La_{1-x}Sr_xMn(III)_{1-y}Mn(IV)_yO_{3+\delta}$ ($\delta = (y - x)/2$). Ideal perovskites have the formula ABO_3. Chemical analyses (1), densities (1), and structure determinations (2–4) of LSM materials have shown that samples with $\delta > 0$ have vacancies at A and B positions, and no interstitial oxygen ions. The notation $La_{1-x}Sr_xMn(III)_{1-y}Mn(IV)_yO_{3+\delta}$ is somewhat misleading, as it indicates an excess of oxygen instead of cation vacancies. It is, however, commonly used and convenient. Unit cell volumes of LSM materials depend linearly upon the oxidation states of manganese. Figure 1 shows the dependence of the room temperature cell volumes upon the oxidation state of the material. The materials were prepared under different partial pressures of oxygen, and

[1]To whom correspondence should be addressed. E-mail: eka@gamma.dou.dk.

0022-4596/98 $25.00

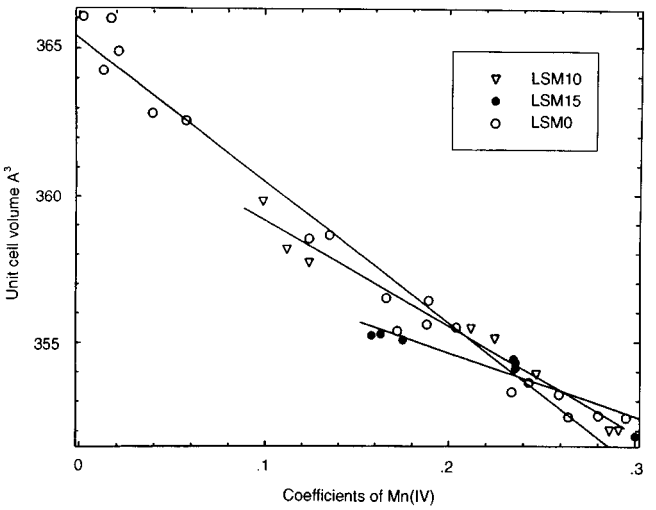

FIG. 1. Room temperature unit cell volumes versus coefficients of Mn(IV) in $La_{1-x}Sr_xMn(III)_{1-y}Mn(IV)_yO_{3+\delta}$ for $x = 0.0, 0.10$, and 0.15.

wet chemical analysis was made to determine the composition and oxidation states. To the extreme left of Fig. 1 the reduced materials are found; to the right the maximum oxidized forms are found. The materials are either orthorhombic (space group *Pnma*) or rhombohedral (space group $R\bar{3}c$, the hexagonal setting was used). The unit cell volumes of the orthorhombic materials have been multiplied by 1.5 to compensate for the different numbers of oxygen ions in the orthorhombic and the hexagonal cells. These are 12 and 18, respectively. A full description of how the data reported in Fig. 1 were obtained is given in (1).

We report kinetic investigation of oxidation of $La_{1-x}Sr_xMn(III)_{1-y}Mn(IV)_yO_{3+\delta}$ for $x = 0.0$, 0.10, and 0.15 (in the following designated LSM0, LSM10, and LSM15, respectively) at four temperatures in the range 700–900°C. At these temperatures the materials are rhombohedral.

EXPERIMENTAL

Sample Preparation

The materials are the same as those used in chemical and structural studies of lanthanum manganates(III) (IV) (1) (5). They were prepared by solid state reactions of acetates of the components (1). Table 1 presents compositions of the reduced and oxidized forms as found by wet chemical analysis.

Time Resolved Powder Diffraction Experiments

The diffraction experiments were performed at the beamline X7B, NSLS, Brookhaven National Laboratory. We have used two types of detectors for the time-resolved diffraction experiments: an INEL CPS 120 curved position sensitive detector and a Translating Imaging Plate Camera (6) (7). A wavelength $\lambda = 1.0987$ Å was used. The reaction chamber was a 0.5-mm diameter quartz capillary mounted on a goniometer head using a ferrule in a Swagelock T-piece (6). The samples were used as synthesized (without fractionation according to particle size). They were loose aggregates of crystallites. The radius of the crystallites were estimated from SEM pictures. The sizes were 0.5–1 μm for LSM0, 0.25 μm for LSM10 (no distinct size distribution), and 0.25–0.4 μm for LSM15. The samples were kept in place in the open capillaries by loose plugs of quartz-glass wool. A two-stringed gas flow system shown in Fig. 2 allowed *in situ* studies of solid-gas reactions under flow conditions. Computer-controlled valves permitted switching between gases during the experiment. The gas used for reduction of the samples was commercial nitrogen (with partial pressure of oxygen 10^{-6} atm). The gases used for oxidation were either dry compressed air or a mixture of 40% nitrogen and 60% oxygen.

The experiments were performed in three consecutive steps. First the reduced form of the sample was heated to the temperature for the experiment in a N_2 gas stream. Then the beam shutter was opened and recording of the diffractograms was started. Finally, when 20–30 diffractograms had been collected, the gas stream was changed to the oxidizing gas while data collection continued. Each diffractogram was accumulated for 30 s, and 10 s was used for data transfer.

RESULTS

Figure 3 shows a small part of the diffractograms recorded for LSM0 at 868°C as a 3D representation, time increases upwards. The time elapsed between two diagrams

TABLE 1
Room Temperature Compositions of Reduced and Oxidized Forms of $La_{1-x}Sr_xMnO_{3+\delta}$ as Found by Wet Chemical Analysis

x	Designation	Formula for reduced form	Formula for oxidized form
0.00	LSM0	$LaMn(III)_{0.99}Mn(IV)_{0.01}O_{3.00}$	$La_{0.99}Mn(III)_{0.73}Mn(IV)_{0.28}O_{3.14}$
0.10	LSM10	$La_{0.90}Sr_{0.10}Mn(III)_{0.89}Mn(IV)_{0.12}O_{3.01}$	$La_{0.90}Sr_{0.10}Mn(III)_{0.71}Mn(IV)_{0.29}O_{3.10}$
0.15	LSM15	$La_{0.84}Sr_{0.15}Mn(III)_{0.85}Mn(IV)_{0.16}O_{3.00}$	$La_{0.85}Sr_{0.15}Mn(III)_{0.71}Mn(IV)_{0.29}O_{3.07}$

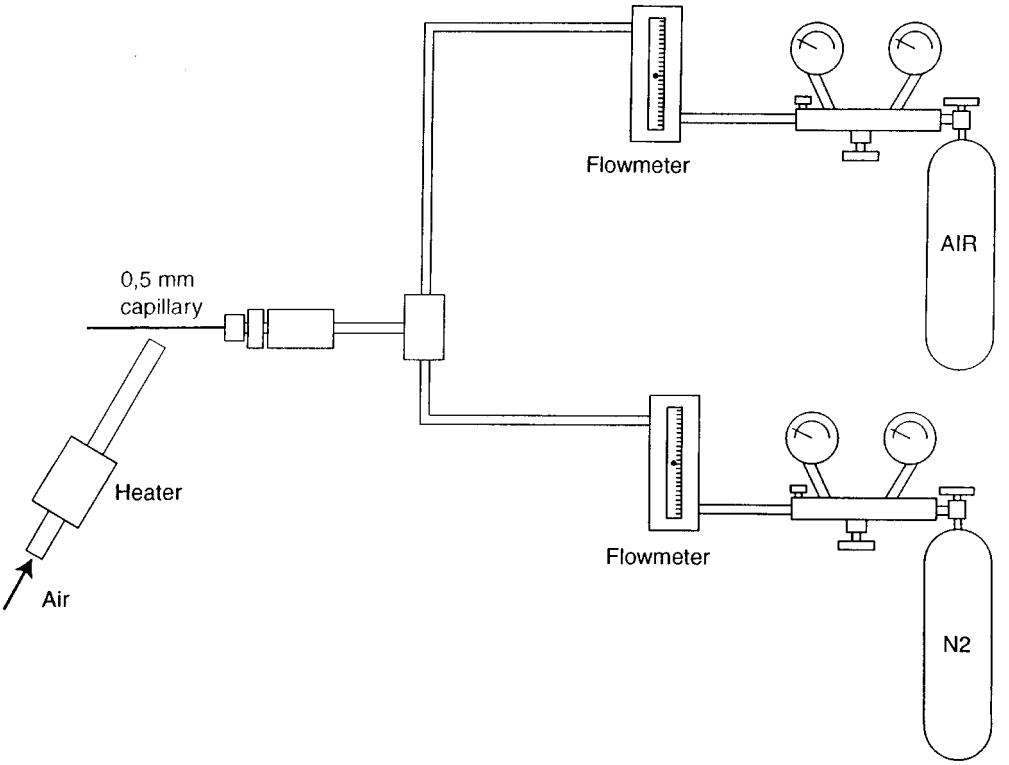

FIG. 2. Two-stringed gas flow system for *in situ* studies of solid-gas reactions under flow conditions. Computer-controlled valves permit switching between gases during the experiment.

is 40 s. The peak shown is the 204 reflection. The time scale of Fig. 3 starts at the bottom and ends at the top diffractogram recorded 48 min after the start. During the first 13 min (until diagram no. 20) the sample was flushed with N_2. During this time the d_{204} value remains constant 1.9688($\pm$2) Å (the diffraction angle $2\theta_{204}$ is constant). Then the gas stream was changed to a mixture of 40% N_2 and 60% O_2. As soon as the gas is changed the d_{204} value starts to decrease (the diffraction angle $2\theta_{204}$ increases). After 48 min the d_{204} is again constant 1.9583($\pm$ 2) Å (the diffraction angle $2\theta_{204}$ is constant).

For interpretation of the obtained diffractograms in terms of kinetics of the oxidation process two methods were used. One is to determine the d value of some nonoverlapping reflection. Only one such reflection (204) exists in the 2θ range covered in the experiments. The d values of this reflection was determined by a fitting procedure using a pseudo-Voigt profile. In the other method the entire diffractogram was indexed and lattice constants refined either using extracted d-spacings and the programme CELLKANT (8), or using profile refinement with the programme ALLHKL (9). All peaks in the diffractograms could be indexed. Selection rules were in accordance with the space group $R\bar{3}c$.

Figure 4 is a presentation of the results of such treatments of diffractograms obtained at 868°C with LSM0. It shows how the d_{204} spacings and unit cell volumes vary with time. The similarity of the curves indicates that both methods for extracting kinetic information from the experiments may be used.

The curves in Fig. 4 were calculated from simple first-order rate equations. For data based on the change of d_{204} values the equation was

$$d_{204}(t) = \Delta d_{204} \times \exp(-k(t - t_0)) + d_{204}(\text{oxidized}),$$

where Δd_{204} is the total change of d_{204} during the oxidation, d_{204}(oxidized) the spacing of fully oxidized LSM0, and t_0 is the time when the gas was changed to 60% O_2.

For data based on unit cell volumes the equation was

$$V(t) = \Delta V \times \exp(-k(t - t_0)) + V(\text{oxidized}),$$

where ΔV is the total change in cell volume between the reduced and the oxidized form, V (oxidized) is the cell volume of fully oxidized LSM0, and t_0 is the time when the gas was changed.

The rate constants k obtained by these two treatments of data for LSM0 are reported in Table 2. Similar treatment of data for LSM10 and LSM15 give the kinetic data reported in Tables 3 and 4.

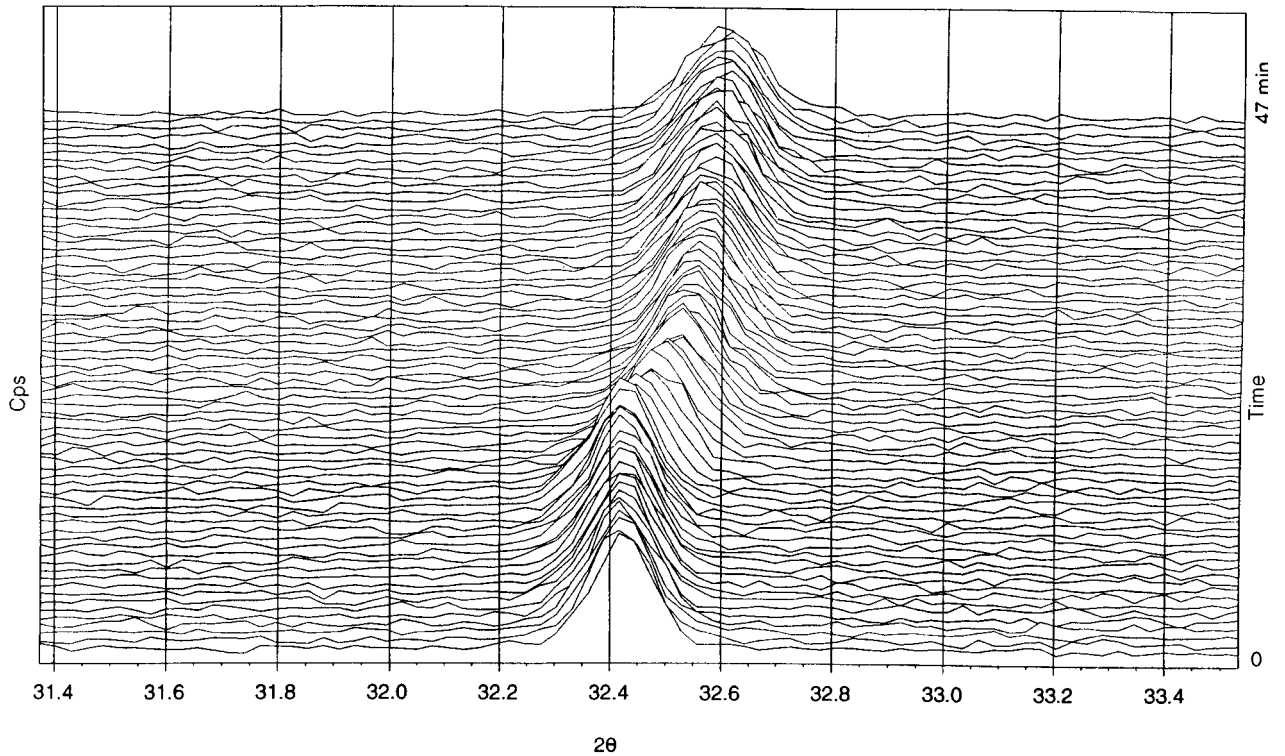

FIG. 3. 3D representation of the change of 2θ values for the 204 reflection of LSM0 at 868°C during oxidation. Time increases upwards. Time elapsed between two diagrams is 40 s. At diagram no. 20 the gas stream was changed from N_2 to a mixture of 40% N_2 and 60% O_2.

Arrhenius plots drawn on the basis of the kinetic data in Tables 2, 3, and 4 are shown in Fig. 5. Within the accuracy of the experiments the four points for each material lie on a straight line. Such behaviour is usually taken as evidence that only one rate-determining step is involved in the process. For LSM0 there are two lines. One is based on $k_{d\ \text{values}}$ the other is based on $k_{\text{cell volumes}}$. The lines have the same slope, and they show that it is of no material consequence whether d values or cell volumes are used for the interpretation of the experiments. From the slopes of the Arrhenius plots activation energies were calculated. These are reported in Table 5.

TABLE 2
Kinetic Data for Oxidation of LSM0

Temperature °C	$k_{d\ \text{values}}$ min^{-1}	$\ln k_{d\ \text{values}}$	k_{volumes} min^{-1}	$\ln k_{\text{volumes}}$	$10000/T\text{K}^{-1}$
733	0.0158	− 4.145	0.0190	− 3.963	9.94
775	0.0249	− 3.694	0.0249	− 3.694	9.54
868	0.1108	− 2.200	0.1217	− 2.160	8.76
900	0.1453	− 1.929	0.1725	− 1.757	8.52

Note. Two sets of data are given. The one based on the time dependence of d_{204} spacings, the other based on cell volumes.

DISCUSSION

The diffractograms recorded during high-temperature oxidation of LSM materials are not simple superpositions of diffraction from reactant material still in reduced form and product in oxidized form. The material remains essentially a single phase. This is clearly borne out by Fig. 3, where the peaks in the middle time range cannot be composed by some combination of the peaks in the first and last diagram. This means that the structural rearrangement at any stage during the oxidation is fast. During the oxidation some line broadening occurs. For reduced LSM0 the full width at half maximum (FWHM) is 0.13° (in 2θ). When the oxidation starts this grows gradually to 0.16°. For LSM15 the growth of the FWHM is less pronounced, from 0.12–0.14°.

TABLE 3
Kinetic Data for Oxidation of LSM10

Temperature °C	$k\ \text{min}^{-1}$	$\ln(k)$	$10000/T\ \text{K}^{-1}$
696	0.0201	− 3.91	10.32
752	0.0435	− 3.14	9.76
816	0.2122	− 1.55	9.18
868	0.5250	− 0.66	8.76

Note. The rate constants are based on unit cell volumes.

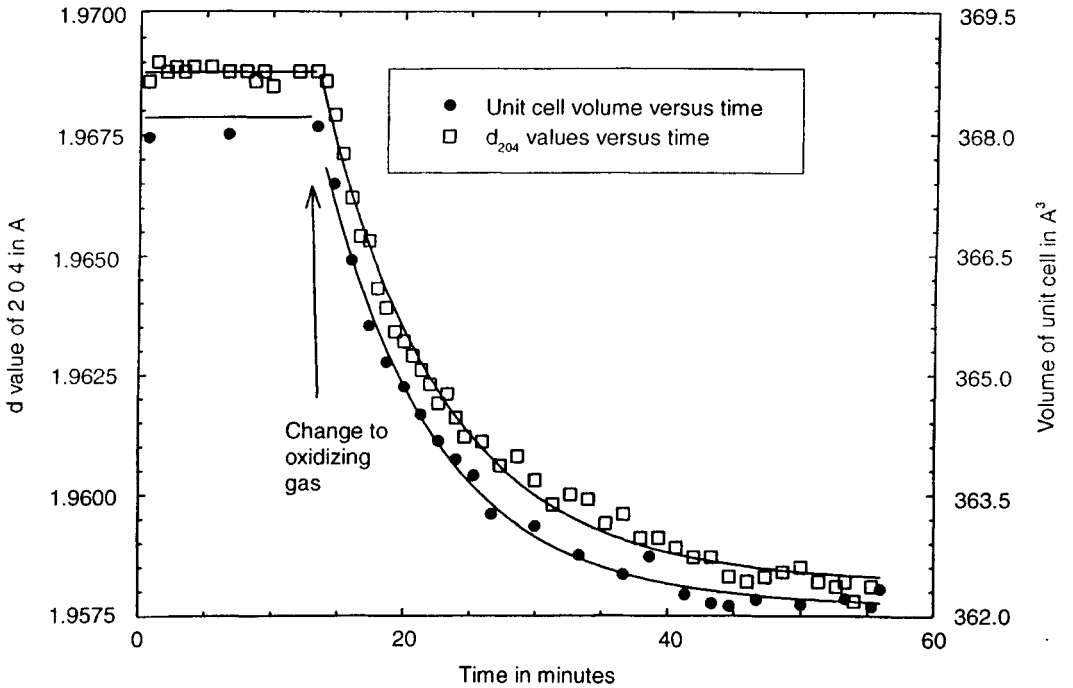

FIG. 4. A graphical presentation of how d_{204} values and unit cell volumes of LSM0 vary with time in an oxidation experiment at 868°C. The curves were calculated from first-order rate equations. For d_{204} value data the equation was: $d_{204}(t) = \Delta d_{204} \times \exp(-k(t-t_0)) + d_{204}$(oxidized), where Δd_{204} is the total change of d_{204} during the oxidation, d_{204}(oxidized) the spacing of fully oxidized LSM0, and t_0 is the time when the gas was changed to 60% O_2. For unit cell volume data the equation was: $V(t) = \Delta V \times \exp(-k(t-t_0)) + V$ (oxidized), where ΔV is the total change in cell volume between the reduced and the oxidized form, V (oxidized) is the cell volume of fully oxidized LSM0, and t_0 is the time when the gas was changed.

Heterogeneous reactions depend upon the particle size of the reactants. Estimated from SEM pictures the LSM0 and LSM15 had particle sizes 3 and 1.3 times larger than the LSM10, respectively. Corrected for the difference in specific surface areas LSM0 and LSM10 show within the accuracy the same rates for the oxidation process. LSM15 has after such correction a slower rate than LSM0 and LSM10.

Kjær *et al.* (10) made thermogravimetric studies in the temperature range 800–1000°C of oxygen transport in exactly the same samples as we used. They interpreted their gravimetric experiments in terms of diffusion of oxygen into spherical particles. By equations given by Jost and Hauffe (11) they calculate diffusion coefficients in the range 10^{-12}–10^{-11} cm^2/s. If we interprete our rate constants for LSM0 and LSM10 using their procedure we get diffusion coefficients 6 times lower than those reported by Kjær *et al.* This deviation is probably within the accuracy of both methods. For LSM15 we calculate diffusion coefficients 10 times lower than Kjær *et al.* The reason for this large discrepancy may stem from that the entire range of δ for this material is diminished to 0.07 and from that the slope of the unit cell volumes versus coefficients of Mn(IV) (shown in Fig. 1) is diminished also. Therefore our accuracy may be low for LSM15. For strontium substituted LSM materials $La_{1-x}Sr_xMnO_{3.00+\delta}$ with $x > 0.25$, δ is zero at oxygen partial pressures between 1 and 10^{-6} atm.

TABLE 4
Kinetic Data for Oxidation of LSM15

Temperature °C	k min^{-1}	ln(k)	$10000/T$ K^{-1}
733	0.005205	− 5.26	9.94
775	0.01096	− 4.51	9.54
868	0.04625	− 3.07	8.76
900	0.08180	− 2.50	8.53

Note. The rate constants are based on d_{204} spacings.

TABLE 5
Activation Energies for the Oxidation of LSM0, LSM10, and LSM15 Obtained from the Slopes of Arrhenius Plots Reported in Fig. 5

	Slope of Arrhenius plot K	Activation energy kJmol^{-1}
LSM0	16.400	136
LSM10	21.500	179
LSM15	19.200	160

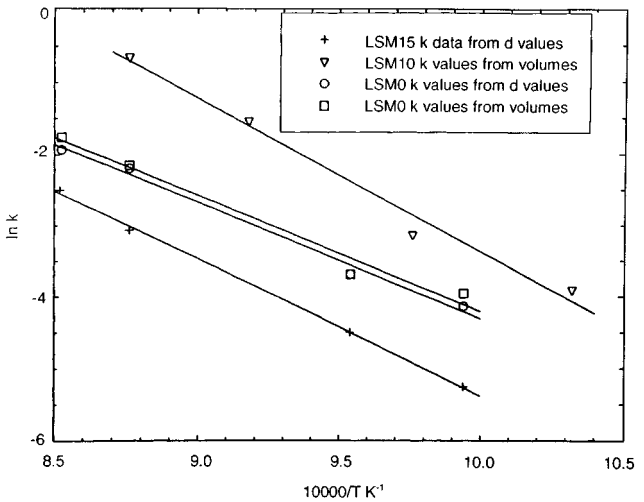

FIG. 5. Arrhenius plots of kinetic data for LSM0, LSM10, and LSM15. The slopes of the curves and activation energies are reported in Table 5.

Yasuda *et al.* (12) determined the ^{18}O diffusion coefficient of LSM materials as function of composition, temperature, and oxygen partial pressure. They found self-diffusion coefficients in a range 10^{-12} to $10^{-11}\,cm^2/s$ and activation energies for diffusion in the range 250–300 $kJmol^{-1}$. These are roughly 2 times larger than the activation energy we found for the oxidation processes. Values of self-diffusion coefficients and chemical diffusion coefficients are connected through an enhancement factor. The temperature coefficient for this factor is not known for LSM materials.

CONCLUSIONS

Time resolved synchrotron X-ray powder diffraction is a versatile tool for kinetic investigation of reaction of solids. It covers a wide range of reaction rates and temperatures. The results presented in this paper have shown that kinetic information of reactions between solids and gases can be obtained by *in situ* time-resolved powder diffraction.

The gas/solid reaction $La_{1-x}Sr_xMnO_{3.00} + \delta/2O_2 \rightarrow La_{1-x}Sr_xMnO_{3.00+\delta}$ (for $x = 0.00, 0.10, 0.15$) was studied. During the reaction the solids remain essentially a single phase. The diffractograms exhibit some line broadening during the oxidation, but not very markedly. This means that the structural rearrangement of the solid during the oxidation is fast.

Corrected for the different specific surface area of the specimens the rate constants show that the oxidation of LSM0 and LSM10 is faster than the oxidation of LSM15. The activation energy for the processes is on average 160 $kJmol^{-1}$.

ACKNOWLEDGMENTS

The work at Odense University was supported by the Danish Ministry of Energy, ELSAM, ELKRAFT (DK-SOFC), by the Albani Brewery Foundation, and by the Danish Natural Science Research Council. The work at Brookhaven National Laboratory was supported under Contract DE-A02-76CH00016 with the U.S. Department of Energy by its Division of Chemical Sciences, Office of Basic Energy Sciences.

REFERENCES

1. I. G. Krogh Andersen, E. Krogh Andersen, P. Norby, and E. Skou, *J. Solid State Chem.* **113,** 320 (1994).
2. B. C. Tofield and W. R. Scott, *J. Solid State Chem.* **10,** 183 (1974).
3. S. Habekost, P. Norby, J. E. Jørgensen, and B. Lebech, *Acta Chem. Scand.* **48,** 377 (1994).
4. J. A. M. Van Roosmalen, "Some Thermochemical Properties of (La, Sr) $MnO_{3+\delta}$ as a Cathode Material for Solid Oxide Fuel Cells," thesis, Amsterdam University, Amsterdam, 1993.
5. P. Norby, E. Krogh Andersen, I. G. Krogh Andersen, and N. H. Andersen, *J. Solid State Chem.* **119,** 191 (1995).
6. P. Norby, *Mater. Sci. Forum* **228–231,** 147 (1996).
7. P. Norby, A. Darovsky, J. C. Hanson, and I. Meschkovsky. ln preparation.
8. N. O. Ersson "Program Cellkant," Institute of Chemistry Uppsala University, Uppsala, Sweden, 1981.
9. G. S. Pawley, *J. Appl. Cryst.* **14,** 357 (1981).
10. J. Kjær, I. G. Krogh Andersen, N. Mogensen, E. Skou, and H. Boye, *in* "Proceedings of the 14th. Risø International Symposium on Material Science: Risø National Laboratory, Roskilde, Denmark, 1993" (F. W. Poulsen, J. J. Bentzen, T. Jacobsen, E. Skou, and M. J. L. Østergård, Eds.), p. 281.
11. W. Jost and K. Hauffe, "Diffusion: Methoden der Messung und Auswertung," p. 74, Dr. Dietrich Steinkopff Verlag, Darmstadt, 1972.
12. I. Yasuda, K. Ogasawara, and M. Hishinuma, *Solid State Ionics* **86–88,** 1197 (1996).